

# Hydrodynamic Analysis of Webbed Foot for a Novel Biomimetic Robotic Duck

Huikang Liu, Zan Li, Yao Hu, Liwei Shi\*, *Member, IEEE*, Shuxiang Guo\*, *Senior Member, IEEE*,  
Xihuan Hou, Huiming Xing, Yu Liu, and Debin Xia

**Abstract**—This paper introduces a biomimetic robotic duck with webbed foot and its hydrodynamic analysis. The swimming gait of the biomimetic robotic duck was designed to implement bionic gait, double-joint cruising gait, and single-joint cruising gait. Through the establishment of the hydrodynamic experimental platform, the gait experiments of different types and different frequencies were carried out. Based on the hydrodynamic analysis, we could lay a foundation for further research on robot motion control, so as to change the overall motion of the robot by adjusting the motion state of the webbed foot.

**Keywords**—Biomimetic robotic duck, webbed foot, gait design, hydrodynamic analysis

## I. INTRODUCTION

In recent years, there has been a growing research on biomimetic amphibious robots as they can move on land, in water or even under water, which excellent amphibious adaptation has attracted many researchers. Because of the amphibious movement ability, this kind of robots can develop for many applications in such fields as the rescue, pollution detection, topographic mapping, archaeological exploration, and resource investigation in the coastal area. Thus, it has great practical value and significance to develop amphibious mobile robot. In addition, the driving structure of amphibious biomimetic robot plays a vital role for the motion in turbulent zones of underwater and transition regions. With the development of amphibious biomimetic robots, many kinds of driving appliances which adopt different propulsion methods have appeared to meet various mission.

Since 2005, Alessandro Crespi et al. designed a series of bio-amphibious salamander robots called *Salamandra robotica* [1-2] which body consists of nine modules and two feet on each side of the body, adopt the CPG (Central Pattern Generator) control model to realize the motion in different environments. In 2005, the amphibious snake-like robot ACM-R5 [3-4] developed by Tokyo Institute of Technology is composed of multiple joints, each of which has two degrees of freedom and can achieve pitch and yaw motion. ACM-R5 can implement tumbling movement using body winding on land and adopt eel-like undulatory propulsion

underwater. In 2012, Junzhi Yu et al. designed a multifunctional amphibious robot, called *AmphiRobot* [5]. The robot is equipped with a new type of hybrid propulsion mechanism that combines wheel with fin structure. The robot can not only achieve flexible wheel-based movements on land, but also perform fish-like or dolphin-like swimming steadily and efficiently underwater, and further switch between the two modes with special rotating devices.

The above series of amphibious robots are inspired by the imitation of fish or snake, all of which use the multi-link structure to complete the flexible movement with a small rotation radius. Most bodies of them are long and narrow, which makes the motion control become complex. Besides, some robots with simple driving structures have been proposed.

In 2007, an amphibious hexapod robot called *AQUA*, developed by Dudek G [6] from McGill University. It used curved legs as the propulsion mechanism on land and propelled underwater through the swing of six paddles. The cockroach-like robot with transformable leg-flipper composite propulsion mechanism called *AmphiHex* [7-8] developed by Shiwu Zhang, which can walk over rugged terrain, operate underwater, and navigate in complex coastal areas. A frog-like robot called *FroBot* was proposed by Yi Yang, which combined the appearance of frog with the characteristics of scooter to create underwater propulsion by opening and closing its legs [9].

According to the application of bionic principles in the different robots, all of above classic robots can be divided into two main categories, including leg-type amphibious robots and snake-like. Most amphibious robots imitated the movement of amphibians such as salamanders, crabs, turtles, cockroaches and snakes. In contrast, the research on amphibious biomimetic robots based on waterfowl is very rare. However, waterfowl also have good adaptability and flexibility both on land and in water. The biological movement characteristics of waterfowl have been in-depth research in multiple theoretical studies [10-15].

Through the observation of waterfowl behavior, we found that their bodies move from side to side because their legs are short and near the tail. But they can swim in the water more efficiently because of the same reason. In nature, the Long-tailed Duck even can dive to a depth of 50 meters. As we all know, the duck species are various and can be seen everywhere, which provides convenient conditions for research. Besides, the duck has a flexible neck, strong flapping wings and webbed feet, which provide inspiration for the design of robot.

Based on bionics principle, our team proposed a novel amphibious biomimetic robotic duck in previous study [16].

\* This research was supported by National Natural Science Foundation of China (61773064, 61503028). This research project was also partly supported by National Key Research and Development Program of China (2017YFB1304401), and Graduate Technological Innovation Project of Beijing Institute of Technology (2018CX10022).

Liwei Shi was with Beijing Institute of Technology, Beijing, China (corresponding author to provide e-mail: [shiliwei@bit.edu.cn](mailto:shiliwei@bit.edu.cn)).

Shuxiang Guo was with Beijing Institute of Technology, Beijing, China (corresponding author to provide e-mail: [guoshuxiang@bit.edu.cn](mailto:guoshuxiang@bit.edu.cn)).

When the robot walks on land, the rear legs are the driving source, and the front leg with the universal wheel is the support. When the robot swims in water, the webbed feet are driven by servo motors to control the periodic opening and closing, which simulates the stroke stage and recovery stage of real creatures moving in water, as shown in Fig.1 [10]. In order to use the novel mechanical webbed feet to control the thrust force generated from the mechanical webbed foot.

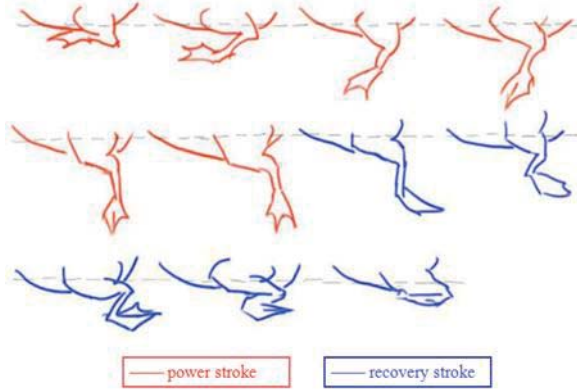


Fig.1. The stroke stage and recovery stage of real creatures moving in water. [10]

The rest of this paper is organized as follows. Section II depicts the biomimetic duck and the novel mechanical webbed feet. The design of robot single-leg underwater gait is shown in Section III. The establishment of hydrodynamic experiment platform and analysis of underwater experiment are introduced in Section IV. Finally, Section V concludes this paper with an outline of future work.

## II. THE BIOMIMETIC ROBOTIC DUCK

The biomimetic robotic duck is shown in Fig.2, mainly divided into head and neck structure, leg structure and shell structure. The leg structure includes driving leg structure, aided leg structure and webbed foot structure, as shown in Fig.3. The driving leg and webbed foot are used to generate underwater propulsion.

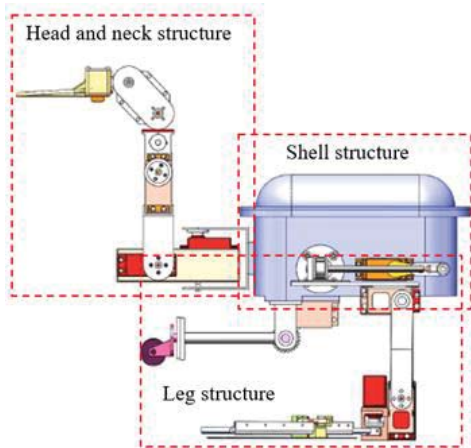


Fig.2. Overall structure of biomimetic robotic duck.

The driving leg is composed of a crank block structure and a two-link structure, which have three degrees of freedom in the vertical plane, as shown in Fig.4. The crank block structure acts as the hip joint, which provide periodic swing for the entire driving leg. The largest advantage of this structure is that the motor does not need to reverse to produce a swing effect. Otherwise, the motor will be damaged easily. The two-link structure is composed of the knee joint, ankle joint and links, which provide more workspace for the webbed foot.

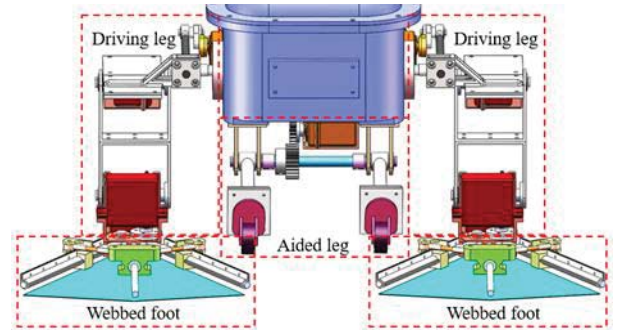


Fig.3. The leg structure of biomimetic robotic duck.

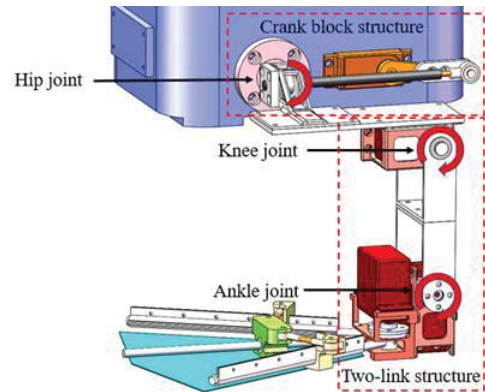


Fig.4. The driving leg of biomimetic robotic duck.

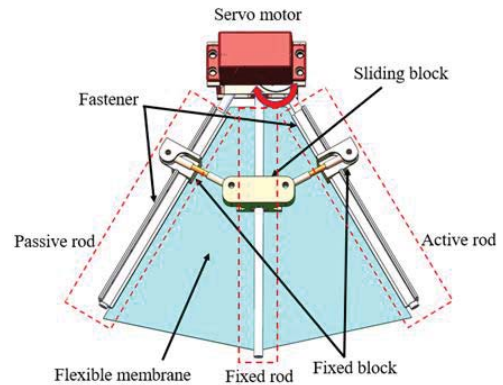


Fig.5. The webbed foot of biomimetic robotic duck.

The webbed foot is the important part for biomimetic robotic duck, due to it is the bottom layer of the control loop.

It is composed of webbed skeleton, flexible membrane, servo motor, as shown in Fig.5. The webbed skeleton has three phalanges, two fixed blocks and one sliding block. The three phalanges are divided into active rod, passive rod and fixed rod. In most other studies [17-20], webbed feet have fixed shapes, such as triangles and rectangles, so they cannot simulate varying underwater movement. For biomimetic robotic duck, the servo motor drives the active lever to control the opening and closing of the whole foot, which simulates the stroke stage and recovery stage of real biological underwater motion. The flexible membrane is attached and clamped by a fastener outside and can be extended to 2-3 times than the initial area. The specific geometric parameters of the novel mechanical webbed feet are shown in Fig.6 and Table I.

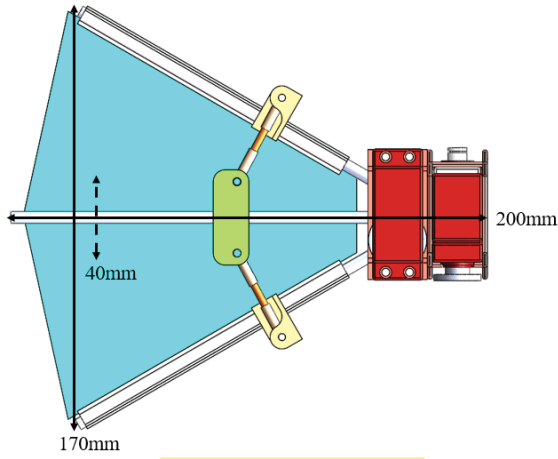


Fig.6. Size of the webbed foot.

TABLE I. WEBBED FOOT GEOMETRIC PARAMETERS

GEOMETRIC PARAMETERS	
Parameter	Value
Length of webbed foot	$L = 200 \text{ mm}$
Chord length range of webbed foot	$W = 40 - 170 \text{ mm}$
Sole area of webbed foot	$S = 6500 - 16000 \text{ mm}^2$
Aspect ratio range of webbed foot	$AR = 0.25 - 1.81$
DOF of leg	$D = 4$

### III. UNDERWATER GAIT DESIGN OF ROBOTIC DUCK

Swimming performance of the biomimetic robotic duck is the key point to be considered. Thus, three kinds of underwater gaits containing bionic gait, single-joint cruising gait and double-joint cruising gait have been designed and introduced, respectively.

#### A. Design of bionic gait

When a waterfowl flaps the feet underwater, their webbed feet move alternately, slowly and slightly. In general, a waterfowl moves forward, backward and turns by flapping their webbed feet in different directions with different forces. The regular of underwater flapping of waterfowl legs is

divided into stroke stage and recovery stage. When the legs and feet of a waterfowl slide back, the flippers are open because of the pressure of water, which increases the contact area with the water, and creates more thrust. In this case, the force between the webbed and the water is conducive to movement. Similarly, when the other webbed foot moves forward, the flipper closes due to the influence of the water, reducing the contact area with the water. In this case, the force between the webbed foot and the water hinders the movement. While, the webbed foot contractions are gentle, which has little impact on the overall movement as the small resistance. Thus, the bionic gait designed for the robot, as shown in Fig.7.

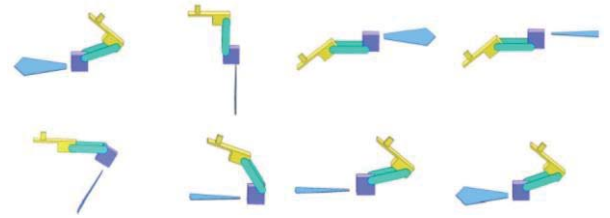


Fig.7. Design of a Bionic Gait.

#### B. Design of double-joint cruising gait

To extend the gait design, a double-joint cruising gait was proposed based on the bionic gait, as shown in Fig.8. For the double-joint cruising gait, swing of the knee joint and the ankle joint provides the propulsion force. The swing amplitude of the two joints are both  $40^\circ$ .

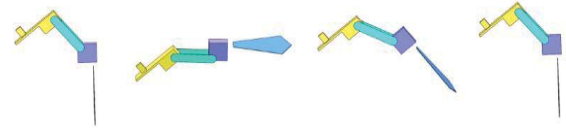


Fig.8. Design of double-joint cruising gait

#### C. Design of single-joint cruising gait

A single-joint cruising gait was proposed, as shown in Fig.9, which provides propulsion force through the crank block structure of the hip joint. Due to the structural limitation, the maximum swing range is fixed at  $\pm 40^\circ$ .



Fig.9. Design of single-joint cruising gait

### IV. EXPERIMENT ANALYSIS

In order to show the motion performance of the biomimetic robotic duck intuitively, the hydrodynamic experiment platform has been designed and assembly. Finally, the experimental results of different gait were obtained.

#### A. Hydrodynamic experiment platform

The force measurement device is shown in Fig.10, which is mainly composed of the hanger connection plate, waterproof tube, force-transmitting bracket, waterproof bottom plate, robot connection frame and force sensor. Among of them, the force sensor adopts the force/torque sensing system of ATI



industrial automation company. This product can measure the force/torque of six degrees of freedom. The maximum force measuring range of the sensor is 65N and the maximum torque measuring range is 5N·m.

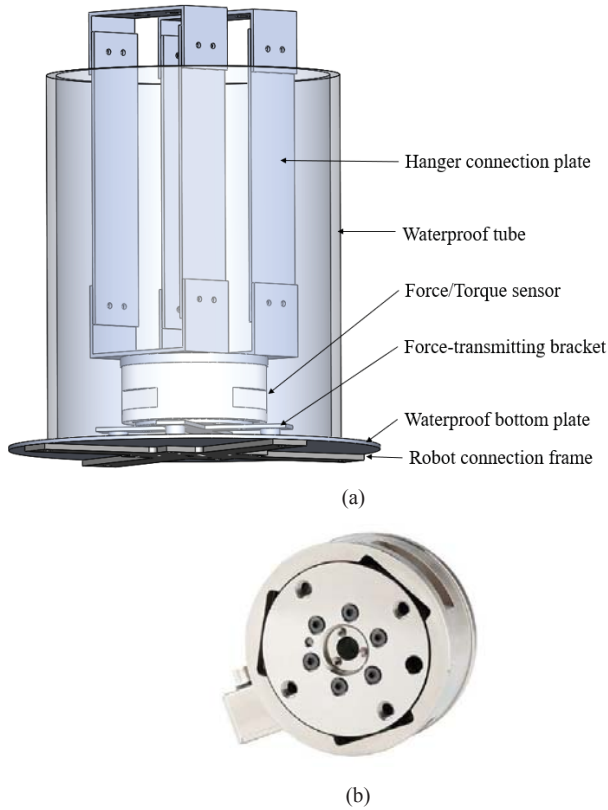


Fig.10. Force measurement device. (a) Assembly drawing of the equipment. (b) ATI force/torque sensor.

After assembling the measurement device, the single leg of the robot is installed on the robot connection frame at the bottom of the device, as shown in Fig.11.

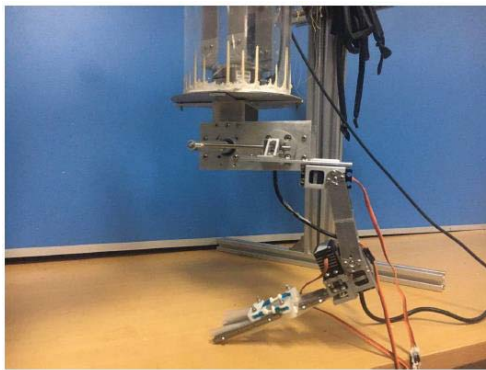


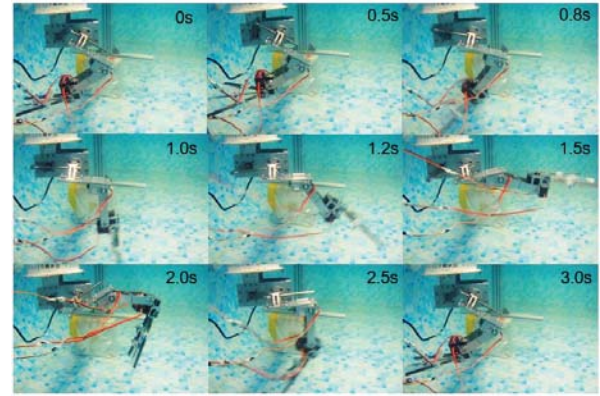
Fig.11. Assembly of single leg and force measurement device

### B. Implementation of swimming gait

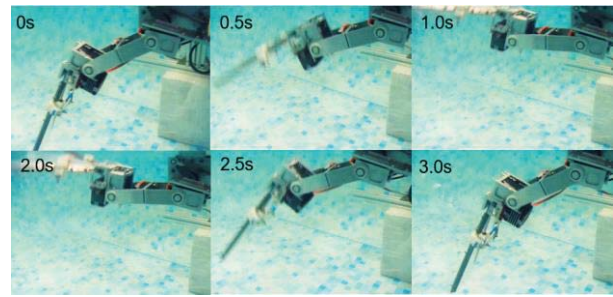
After completing the gait design, the bionic gait, double-joint cruising gait and single-joint cruising gait on one side leg of the robot are realized by controlling each joint motor.

In the experiment, water resistance always exists in the swinging process of the driving leg, and the higher swinging speed will cause the greater resistance. Therefore, the swing

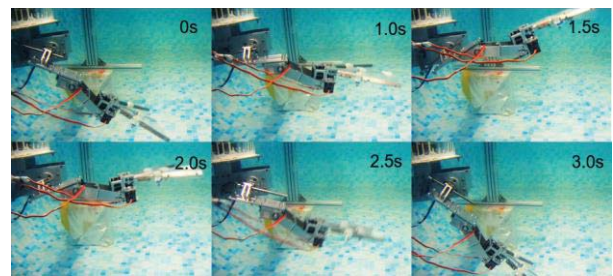
frequency of the robot leg should not be too fast, otherwise the motor driving the mechanical leg will be out of step and unable to rotate to the designated position. Finally, we performed the bionic gait with a period of 2s,3s,4s, double-joint cruising gait with a period of 1s,2s,3s, and single-joint cruising gait with a period of 3s,4s. As shown in Fig.12, the three gaits are implemented with a swing period of 3s.



(a)



(b)



(c)

Fig.12. Realize the gait of biomimetic robotic duck. (a) Bionic gait. (b) Double-joint cruising gait. (c) Single-joint cruising gait

### C. Experimental analysis of swimming gait

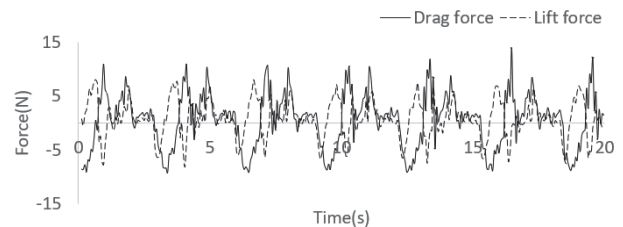


Fig.12. The bionic gait with a period of 3s for 20s.

First, the bionic gait was analyzed with a period of 3s for 20s. The calculation results obtained by force sensor are shown in the Fig.12. It can be seen that there are six complete cycles. The data of each cycle are compared, and the trim mean was processed to generate the drag and lift force curves of one cycle.

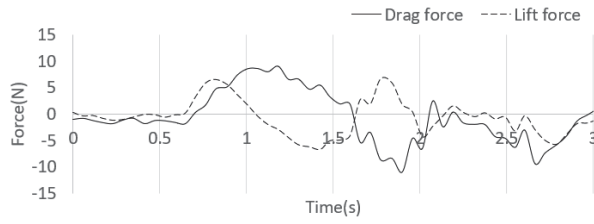


Fig.13. The drag and lift curves of one cycle of the bionic gait.

As shown in Fig.13, the time period within 0-0.6s represents that the robot is opening the webbed foot; 0.6-1.1s is the action to swing the leg downwards; 1.1-1.6s is the action to swing the leg upwards; 1.6-2s is the action to closing the webbed foot; and 2-3s is the action in recovery stage. Among these stage, both the leg downwards and upwards stages produce the drag force. The other stages are only to recovery the leg movement to ensure the kick motion continue running in next period.

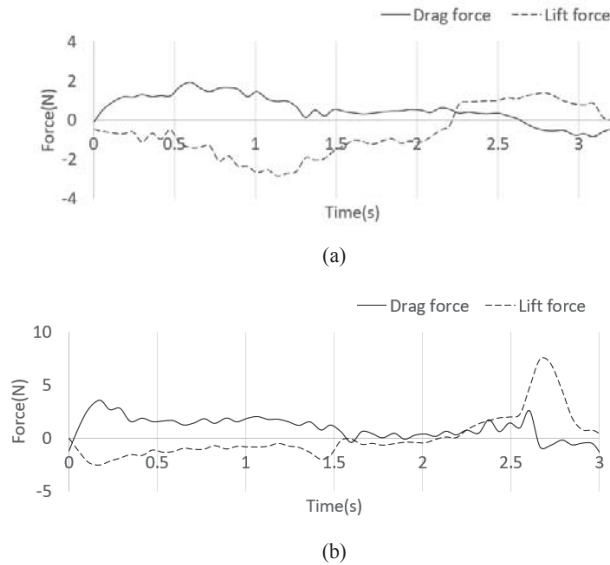


Fig.14. The drag and lift curves of one cycle of the double-joint cruising gait and single-joint cruising gait.

The gait of double-joint cruising gait was analyzed with the same method. As shown in Fig14(a), 0-2.2s is the upward swing of the robot leg, and 2.2-3s is the recovery stage of the leg. The result of single-joint cruising gait was shown in Fig14(b). The 0-1.6s is the upward swing of the leg, and 1.6-3s is the recovery stage.

The drag force and lift force under different gaits of the robot were compared within one period. For the bionic gait, the maximum drag force is larger, but the drag force accounts for a small proportion of time in one cycle. For the double-joint cruising gait provides a larger proportion of propulsion time than the bionic gait, but the maximum drag force is relatively small. However, the single-joint cruising

gait could provide maximum drag force similar to that of double-joint cruising gait. More importantly, it can provide more sustained propulsion than any other gaits. Considering lift force, the bionic gait changed the direction of lift force three times in one period, and the other two cruising gaits changed the direction only once. According to the vibration from upward and downward directions to compare the performance of the two kinds of gait. The cruising gaits are more suitable for the mechanical duck to swim.

As shown in Fig.15, the proportion of robot propulsion force is relatively larger in the 0.5Hz bionic gait than 0.25Hz. But the propulsive resistance in recovery stage is larger. Thus, the time ratio of propulsion force under the condition of 0.5Hz can be further increased, and the 0.25Hz swing needs to slow down in foot retraction process to reduce resistance.

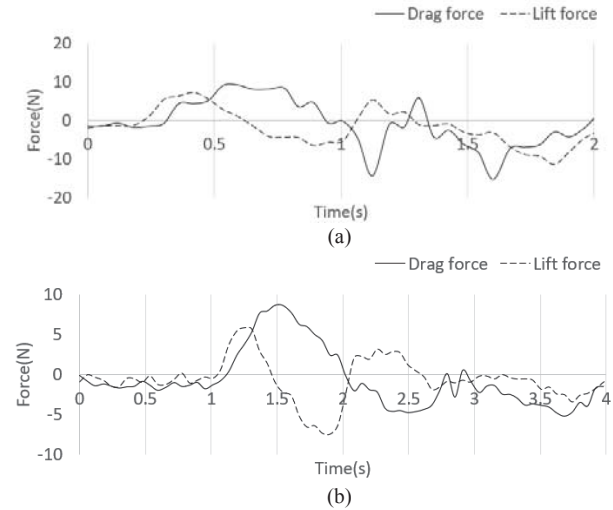


Fig.15. The drag and lift curves of different frequencies of the bionic gait. (a) The 0.5Hz bionic gait. (b) The 0.25Hz bionic gait.

As shown in Fig.16, the proportion of robot propulsion force is relatively larger in the 1Hz double-joint cruising gait than 0.5Hz. The maximum propulsive force is larger, but the propulsive resistance during the recovery process is also larger. So the leg swing needs to slow down during the recovery process to reduce the resistance. In addition, the propulsion force generated is not obvious under 0.25Hz.

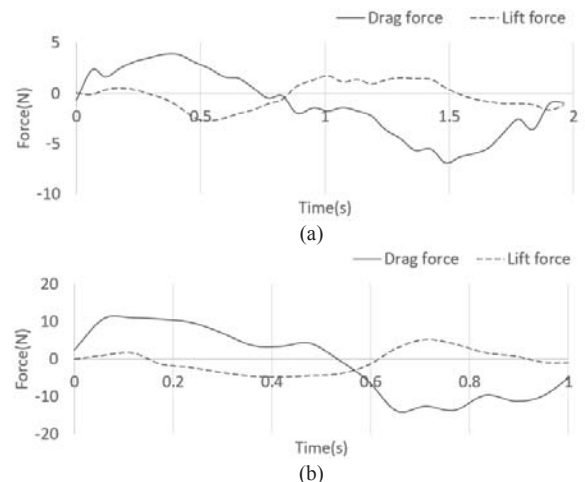


Fig.16. The drag and lift curves of different frequencies of the double-joint cruising gait. (a) The 0.5Hz double-joint cruising gait. (b) The 0.25Hz double-joint cruising gait.

As shown in Fig.17, 0.33Hz single-joint cruising gait can produce greater propulsion force than 0.25Hz, and more stable and continuous.

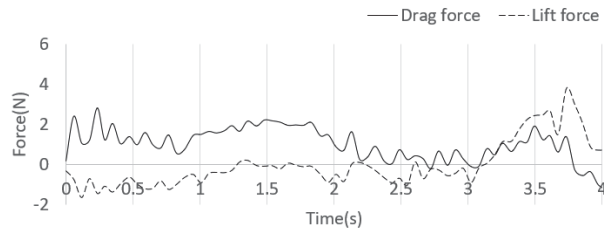


Fig.17. The drag and lift curves of 0.25Hz single-joint cruising gait.

Furthermore, our team have some realistic basis on selecting the range of operational periods. Because of the limitation of rotation speed and torque of stepping motors on the leg, the upper limitation of operational frequency of bionic gait and cruising gait is 0.5Hz. The frequency is better not lower than 0.25Hz, otherwise the drag force is quite small, and make no sense for biomimetic duck to swim. The frequency need reach a value near 0.33Hz, which provides an optimal swimming performance.

Analysis of different gaits and different frequencies can provide the most direct reference for the implementation and improvement on robot motion. The three gaits could be applied in different application scenarios. Among them, the bionic gait can be used for starting, providing the maximum initial propulsion and obtaining the maximum initial speed. The double-joint cruising gait is used for the transition of gait, which has relatively large propulsive force and short period, that can be used for acceleration. Unlike other gaits provide intermittent propulsion, the single-joint cruising gait provides sustained thrust with little resistance, which can provide a steady speed for the robot.

## V. CONCLUSION

This paper has introduced the biomimetic robotic duck and its performance test platform. The hydrodynamics measurement results verify that the robot can complete the designed gait trajectory in water and the propulsion performance of the robot webbed foot is analyzed. The analysis reflects the application effect of different gait on robot. The maximum drag force of bionic gait is more larger, so it is very suitable for bionic duck to accelerate in a short time. Although the maximum drag force of cruising gait is a bit small, the average drag force and lift force are more stable. It is satisfied for bionic duck to maintain its speed in a long time. Finally, it can provide valuable ideas for further test each gait separately in this paper, so the current test results can only explain the characteristics of each gait. However, there is a coordination and transition relationship between each gait in practical application, and only one gait cannot achieve good results in practical application. According to the chapter IV, the swimming strategy is: first, the bionic gait is used to accelerate, then use cruising gate to maintain its speed. Therefore, the underwater gaits can be further optimized in the subsequent research and applied to the whole machine free motion, so as to study the effect of combined gait on

robot and obtain the motion mode closest to the biomimetic performance.

## REFERENCES

- [1] G. O. Young, "Synthetic structure of industrial plastics (Book style with paper title and editor)," in *Plastics*, 2nd ed. vol. 3, J. Peters, Ed. New York: McGraw-Hill, 1964, pp. 15–64.
- [2] W.-K. Chen, *Linear Networks and Systems* (Book style). Belmont, CA: Wadsworth, 1993, pp. 123–135.
- [3] H. Poor, *An Introduction to Signal Detection and Estimation*. New York: Springer-Verlag, 1985, ch. 4.
- [4] B. Smith, "An approach to graphs of linear forms (Unpublished work style)," unpublished.
- [5] E. H. Miller, "A note on reflector arrays (Periodical style—Accepted for publication)," *IEEE Trans. Antennas Propagat.*, to be published.
- [6] J. Wang, "Fundamentals of erbium-doped fiber amplifiers arrays (Periodical style—Submitted for publication)," *IEEE J. Quantum Electron.*, submitted for publication.
- [7] C. J. Kaufman, Rocky Mountain Research Lab., Boulder, CO, private communication, May 1995.
- [8] Y. Yorozu, M. Hirano, K. Oka, and Y. Tagawa, "Electron spectroscopy studies on magneto-optical media and plastic substrate interfaces(Translation Journals style)," *IEEE Transl. J. Magn.Jpn.*, vol. 2, Aug. 1987, pp. 740–741 [*Dig. 9<sup>th</sup> Annu. Conf. Magnetism Japan*, 1982, p. 301].
- [9] M. Young, *The Technical Writers Handbook*. Mill Valley, CA: University Science, 1989.
- [10] J. U. Duncombe, "Infrared navigation—Part I: An assessment of feasibility (Periodical style)," *IEEE Trans. Electron Devices*, vol. ED-11, pp. 34–39, Jan. 1959.
- [11] S. Chen, B. Mulgrew, and P. M. Grant, "A clustering technique for digital communications channel equalization using radial basis function networks," *IEEE Trans. Neural Networks*, vol. 4, pp. 570–578, July 1993.
- [12] R. W. Lucky, "Automatic equalization for digital communication," *Bell Syst. Tech. J.*, vol. 44, no. 4, pp. 547–588, Apr. 1965.
- [13] S. P. Bingulac, "On the compatibility of adaptive controllers (Published Conference Proceedings style)," in *Proc. 4th Annu. Allerton Conf. Circuits and Systems Theory*, New York, 1994, pp. 8–16.
- [14] G. R. Faulhaber, "Design of service systems with priority reservation," in *Conf. Rec. 1995 IEEE Int. Conf. Communications*, pp. 3–8.
- [15] W. D. Doyle, "Magnetization reversal in films with biaxial anisotropy," in *1987 Proc. INTERMAG Conf.*, pp. 2.2-1–2.2-6.
- [16] G. W. Juette and L. E. Zeffanella, "Radio noise currents n short sections on bundle conductors (Presented Conference Paper style)," presented at the IEEE Summer power Meeting, Dallas, TX, June 22–27, 1990, Paper 90 SM 690-0 PWRs.
- [17] J. G. Kreifeldt, "An analysis of surface-detected EMG as an amplitude-modulated noise," presented at the 1989 Int. Conf. Medicine and Biological Engineering, Chicago, IL.
- [18] J. Williams, "Narrow-band analyzer (Thesis or Dissertation style)," Ph.D. dissertation, Dept. Elect. Eng., Harvard Univ., Cambridge, MA, 1993.
- [19] N. Kawasaki, "Parametric study of thermal and chemical nonequilibrium nozzle flow," M.S. thesis, Dept. Electron. Eng., Osaka Univ., Osaka, Japan, 1993.
- [20] J. P. Wilkinson, "Nonlinear resonant circuit devices (Patent style)," U.S. Patent 3 624 12, July 16, 1990.